

Kenji NAKAYAMA and Teruchika SEKI

Transmission Div., NEC Corporation
Kawasaki-Shi, 211 JAPAN

ABSTRACT

A systematic design method for multirate filters which play an important role in sampling rate conversion techniques is proposed in this paper. Purpose of the proposed approach is directed toward circuit complexity reductions. A circuit complexity evaluating measure including quantization error effects is introduced. A transfer function is divided into three factors as follows: $P_1(z)P_2(z)/Q(z^M)$. Optimum characteristics of these factors are discussed which minimize the above measure.

INTRODUCTION

In digital signal processing systems, sampling rate conversion techniques which are decimation and interpolation play an important role. Filters used in the above field are usually called "multirate filters" whose input and output signals have different sampling rates [1], [2].

Several design approaches have been reported [3] - [6]. However, design approaches which are directed toward minimizing the circuit complexity including quantization error effects have not been well discussed.

In this paper, a systematic design method is proposed, which approximate a frequency response in the mini-max sense [7]. Furthermore, a simultaneous frequency and time domain approximation method based on the algorithm reported by [8] is also proposed. A circuit complexity evaluating measure including quantization error effects is introduced. A transfer function is divided into the following three factors, $H(z) = P_1(z)P_2(z)/Q(z^M)$. Optimum characteristics of these factors are discussed which minimize the above measure.

TRANSFER FUNCTION AND CIRCUIT CONFIGURATION

Transfer functions for the multirate filters are classified into the following two categories, Polyphase Filter [3], [4]:

$$H(z) = \sum_{i=0}^{M-1} z^{-i} H_i(z^M), \quad z = e^{j\omega T}, \quad T = 1/f_s \quad (1)$$

where, f_s is a sampling frequency.

Multistage Filter [5], [6]:

$$H(z) = \prod_{k=0}^{K-1} H_k(z_k) \quad (2a)$$

$$z_k = z^{M_k}, \quad M_k: \text{positive integer.} \quad (2b)$$

Since each $H_k(z_k)$ is independently optimized in a partial frequency band in the multistage filter, a filter response in a whole frequency range is not optimized in some sense such as the L_p norm or mini-max criteria. On the other hand, the polyphase filter approach can optimize $H(z)$ over a whole frequency range [4]. For this reason, the polyphase filter method is basically employed in this paper.

When $H(z)$ takes a finite impulse response (FIR) form, sub-functions $H_i(z^M)$ ($i=0 \sim M-1$) can be easily obtained merely by decimating the $H(z)$ coefficients. Bellanger et al proposed the expanding method for infinite impulse response (IIR) transfer functions [4]. This method is called Bellanger's method here. The transfer function approximation and expansion procedures in this method are very simple. However, the poles and zeros, which appear in the stopband after the transfer function expansion, exactly cancel each other with infinite precision coefficients, and cause the following problems.

- (i) Exactly cancelled poles and zeros do not contribute to optimize stopband attenuation.
- (ii) The cancellation is easily broken by coefficient quantization, and large stopband attenuation deviations result.

The transfer function form by Eq. (3) is, therefore, employed to be approximated in the proposed method in order to remove the pole zero location constraints [7], [9].

$$H(z) = \frac{P(z)}{Q(z^M)} \quad (3)$$

APPROXIMATION ALGORITHM

The denominator $Q(z^M)$ is a periodical function with a period of f_s/M Hz, thus it does not contribute to optimizing stopband attenuation. Therefore, the numerator $P(z)$ is used for this purpose, and $Q(z^M)$ is mainly utilized to optimize passband amplitude.

The multirate filters are usually narrow band filters. For instance M values are $14 \sim 72$ and $4 \sim 6$ for TDM-FDM transmultiplexers [10] and data modems [11], respectively. This means that a high-order function must be required for $P(z)$. Furthermore, zeros located in the passband are required to approximate a time response, in other words, to equalize amplitude and phase distortions caused by $Q(z^M)$. These zeros are not always located at the

mirror image positions. Furthermore, taking computational efficiency into account as described later, the numerator $P(z)$ is separated into two factors $P_1(z)$ and $P_2(z)$ which have linear phase and non-linear phase characteristics, respectively. $P_1(z)$ consists of the zeros located on the unit circle in the stopband and is used for optimizing stopband attenuation. The $P_2(z)$ zeros are located in the passband.

Considering the above discussions, the following approximation algorithm is proposed.

$P_1(z)$: Since the order of $P_1(z)$ is usually high, and the optimum zeros are located on the unit circle for stopband attenuation realization, a linear programming method, such as the Remez-exchange method [12], can be efficiently applied with short computing time.

$P_2(z)/Q(z^M)$: $P_2(z)$ is utilized for time response optimization, and $Q(z^M)$ is utilized for the passband amplitude shaping. The simultaneous frequency and time domain approximation of $P_2(z)/Q(z^M)$ is carried out through the algorithm reported by [8]. $P_1(z)$ is dealt with as a fixed weighting function. Since the frequency bands optimized using $P_1(z)$ and $P_2(z)/Q(z^M)$ are completely separated, that is the stopband and passband, respectively, the global optimum solution can be obtained through a few of iteration steps even though they are independently optimized.

The proposed design flow chart is shown in Fig. 1.

CIRCUIT COMPLEXITY EVALUATING MEASURE

Circuit complexity evaluation, taking into account quantization errors in coefficients and internal signals, is discussed here. The following discussions are carried out under the assumptions of the structure shown in Fig. 2, and of a direct form for $P_1(z^M)$ and $Q(z^M)$. Letting $\Delta H(z)$ be the deviation function of $H(z)$ caused by the coefficient quantization errors, its maximum value can be expressed as

$$\max_{\omega} |\Delta H(e^{j\omega})|^2 = \frac{\Delta_c^2}{12} \left\{ \frac{N_n}{|Q(e^{jM\omega+p})|^2} + N_d - 1 \right\} \quad (4)$$

where, Δ_c corresponds to the least significant bit (LSB) of coefficient wordlengths, f_{+p} is a cutoff frequency, N_n and N_d are numerator and denominator orders, respectively. The detailed derivation of Eq. (4) is given at the end of this section. Excess coefficient wordlengths, which correspond to $\max_{\omega} |\Delta H(e^{j\omega})|$, can be expressed as

$$\Delta W^c = \frac{1}{2} \log_2 \left\{ \frac{\max_{\omega} |\Delta H(e^{j\omega})|^2}{(\Delta_c^2/12)} \right\}. \quad (5)$$

Furthermore, the filter output roundoff noise, caused by rounding off multiplier outputs, can be obtained as

$$N_{out} = \frac{\Delta_d^2}{12} \left\{ \frac{N_d - 1}{|Q(e^{jM\omega+p})|^2} + N_n \right\} \quad (6)$$

where, Δ_d corresponds to LSB of internal signals. Excess data wordlengths are expressed as

$$\Delta W^d = \frac{1}{2} \log_2 \left\{ \frac{N_{out}}{(\Delta_d^2/12)} \right\}. \quad (7)$$

The following two measures for both single-channel and multi-channel systems are introduced, taking the above quantization error effects into account. Single-channel:

$$\eta(1) = (N_n + N_d - 1)(W_0^c + \Delta W^c)(W_0^d + \Delta W^d). \quad (8)$$

Multi-channel:

$$\eta(2) = \{N_n + M(N_d - 1)\}(W_0^c + \Delta W^c)(W_0^d + \Delta W^d) \quad (9)$$

where W_0^c and W_0^d are common wordlengths to satisfy the specified roundoff noise level. The denominator $Q(z^M)$ is employed for each channel.

Proof of Eq. (4)

From the assumption given previously, a transfer function $H(z)$ is expressed as

$$H(z) = \frac{\sum_{n=0}^{N_n-1} a_n z^{-n}}{\sum_{n=0}^{N_d-1} b_n z^{-nM}}, \quad b_0 = 1. \quad (10)$$

Letting Δa_n and Δb_n be quantization errors for a_n and b_n , respectively, the transfer function error $\Delta H(z)$ can be expressed, assuming Δa_n and Δb_n are very small, and using a first-order approximate equation as follows:

$$\Delta H(z) \cong \frac{\Delta P(z)}{Q(z^M)} - H(z) \cdot \Delta Q(z^M) \quad (11)$$

where

$$\Delta P(z) = \sum_{n=0}^{N_n-1} \Delta a_n z^{-n} \quad (12a)$$

$$\Delta Q(z^M) = \sum_{n=1}^{N_d-1} \Delta b_n z^{-nM}. \quad (12b)$$

$\Delta P(z)$ and $\Delta Q(z^M)$ can be statistically evaluated by Eqs. (13a) and (13b) [13],

$$|\Delta P(e^{j\omega})|^2 = \frac{\Delta_c^2}{12} N_n \quad (13a)$$

$$|\Delta Q(e^{jM\omega})|^2 = \frac{\Delta_c^2}{12} (N_d - 1) \quad (13b)$$

where Δa_n and Δb_n are assumed to be uniformly distributed in the region $[-\Delta_c/2, \Delta_c/2]$ and to be white noise. Since $\Delta P(z)$ and $\Delta Q(z^M)$ are independent from each other, $\Delta H(z)$ can be estimated by

$$|\Delta H(e^{j\omega})|^2 \cong \frac{\Delta_c^2}{12} \left\{ \frac{N_n}{|Q(e^{jM\omega+p})|^2} + |H(e^{j\omega})|^2 (N_d - 1) \right\}. \quad (14)$$

The maximum value of Eq. (14) is determined by $\max_{\omega} |Q(e^{jM\omega+p})|^{-1}$. Considering the following relation and the $P_1(z)$ amplitude characteristic

$$\left| \frac{P_1(e^{j\omega})}{Q(e^{jM\omega+p})} \right| \cong 1, \quad 0 \leq \omega \leq \omega_{+p}, \quad (15)$$

$|Q(e^{jM\omega+p})|^{-1}$ takes the maximum value at $\omega = \omega_{+p}$ which is the passband edge. Therefore,

$$\max_{\omega} |\Delta H(e^{j\omega})|^2 \cong \frac{\Delta_c^2}{12} \left\{ \frac{N_n}{|Q(e^{jM\omega+p})|^2} + N_d - 1 \right\} \quad (16a)$$

where

$$|H(e^{j\omega+p})| \cong 1. \quad (16b)$$

Q. E. D.

CHARACTERISTICS OF THREE FACTORS TO MINIMIZE $\eta(1)$ AND $\eta(2)$

From Eqs. (8) and (9), $\eta(1)$ and $\eta(2)$ are determined by N_n , N_d and $|Q(e^{jM\omega+p})|^{-1}$. Their relations are given in the following. $|Q(e^{jM\omega+p})|^{-1}$ can be approximately estimated by

$$|Q(e^{jM\omega+p})|^{-1} \cong \prod_{i=0}^I \frac{\sin\{\frac{\pi}{f_s}(f_c - f_{+p}^N + i\Delta f)\}}{\sin\{\frac{\pi}{f_s}(f_c - f_{+p}^N + i\Delta f)\}} \quad (17a)$$

where

$$\Delta f = \frac{f_s - 2f_c}{N} \quad (17b)$$

and the integer I satisfies the following condition

$$\frac{\sin\{\frac{\pi}{f_s}(f_c - f_{+p}^N + I\Delta f)\}}{\sin\{\frac{\pi}{f_s}(f_c - f_{+p}^N + \Delta f)\}} \cong 1. \quad (17c)$$

where, a frequency f_{+p}^N is a cutoff frequency of $P_1(z)$, and satisfies $f_{+p}^N \leq f_{+p}$. A frequency f_c indicates the lower stopband edge. Furthermore, Eq. (17a) is approximately expressed as

$$|Q(e^{jM\omega+p})|^{-1} \cong \prod_{i=0}^I \frac{f_c - f_{+p}^N + i\Delta f}{f_c - f_{+p}^N + i\Delta f}. \quad (18)$$

N_n is proportional to f_s [14],

$$N_n \cong Kf_s, \quad K: \text{constant}. \quad (19)$$

From this relation, Δf by Eq. (17b) becomes

$$\Delta f \cong \frac{1}{K}, \quad 2f_c \ll f_s. \quad (20)$$

From Eqs. (18) and (20), $|Q(e^{jM\omega+p})|^{-1}$ is independent from M, and is determined only by f_c , f_{+p} and f_{+p}^N . An example for this relation is shown in Fig. 3, where A_{+p} is

$$A_{+p} = 20 \log |Q(e^{jM\omega+p})|^{-1}. \quad (21)$$

The $P_1(z)$ order $N_n^{(1)}$ for the given f_{+p}^N can be obtained by the design chart compiled by Rabiner et al [14]. $|Q(e^{jM\omega+p})|^{-1}$ for the given f_{+p}^N is also estimated using Eq. (18). An example is shown in Fig. 4, and the Eq. (18) efficiency can be confirmed. Using these results, the relation between $N_n^{(1)}$ and $\eta(1)$, $\eta(2)$ is obtained, and the optimum f_{+p}^N to minimize $\eta(1)$ and $\eta(2)$ can be derived. An example corresponding to Fig. 4 is shown in Fig. 5. From this figure, the smallest f_{+p}^N becomes the optimum value.

DESIGN EXAMPLES

Frequency Response Specified

Design parameters are given in Table 1. The frequency responses designed through the proposed method is shown in Fig. 6. The results and the

circuit complexities for three methods are listed in Table 2.

Frequency and Time Responses Specified

Design parameters are listed in Table 3. Minimum mean square error approximation based on the linear equation method [8], is employed for simultaneous passband amplitude and time response approximation. The obtained frequency and time responses are illustrated in Figs. 7(a) and (b), respectively. Figure 8 illustrates the resulting pole-zero locations. Table 4 shows results and circuit complexities for the FIR filter and the proposed approaches.

From these results, it is recognized that the proposed design approach can reduce the circuit complexities from the conventional methods.

CONCLUSION

A systematic design method for the multirate filters is proposed. It can reduce the circuit complexity including quantization error effects using lower-order transfer functions than that by the conventional methods. Several design examples show the proposed approach efficiency.

REFERENCES

- [1] R.W.Schafer et al, "A digital signal processing approach to interpolation," Proc.IEEE vol.61, pp. 692-702, June 1973.
- [2] R.E.Crochiere et al, "Interpolation and decimation of digital signal-A tutorial review," Proc. IEEE vol.69, pp.300-331, Mar.1981.
- [3] M.Bellanger et al, "TDM-FDM transmultiplexer: Digital polyphase and FFT," IEEE Trans.vol.COM-22, pp.1199-1205, Sept.1974.
- [4] M.G.Bellanger et al, "Digital filtering by polyphase network: Application to sample-rate alteration and filter bank," IEEE Trans.vol.ASSP-24, pp. 109-114, Apr.1976.
- [5] S.Darlington, "On digital single-side-band modulators," IEEE Trans. vol.CT-17, pp.409-414, Aug.1970.
- [6] M.G.Bellanger et al, "Interpolation, extrapolation, and reduction of computation speed in digital filters," IEEE Trans.vol.ASSP-22, Aug.1974.
- [7] K.Nakayama, "A design method for multirate filters (in Japanese)," IECE of Japan, Rept.Tech.Meeting, vol.CAS81-90, pp.31-38, Dec.1981.
- [8] K.Nakayama, "A simultaneous frequency and time domain approximation method for discrete-time filters," Proc.IEEE ISCAS'82, pp.354-357, May 1982.
- [9] T.A.Ramstad, "Some considerations on coefficient sensitivity and noise in direct form IIR interpolators and decimators," Proc.IEEE ICASSP'79, pp. 371-374, 1979.
- [10] R.Maruta et al, "24 and 120-channel transmultiplexers built with new digital signal processing LSI's," IEEE Trans.vol.COM-30, July 1982.
- [11] K.Watanabe et al, "A 4800 bit/s microprocessor data modem," IEEE Trans.vol.COM-26, May 1978.
- [12] T.W.Parks et al, "Chebyshev approximation for non-recursive digital filters with linear phase," IEEE Trans.vol.CT-19, pp.189-194, Mar.1972.
- [13] D.S.K.Chan et al, "Analysis of quantization errors in the direct form for finite impulse response digital filters," IEEE Trans.vol.AU-21, Aug.1973.
- [14] L.R.Rabiner et al, Theory and Application of digital Signal Processing, Prentice-Hall, Inc., 1975.

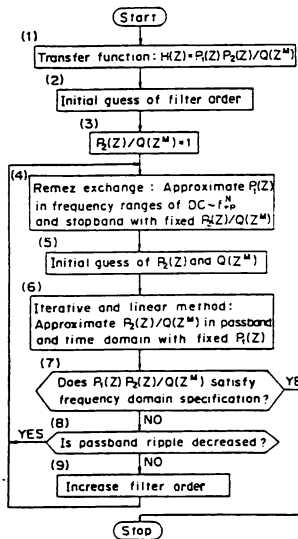


Fig. 1 Design flow chart.

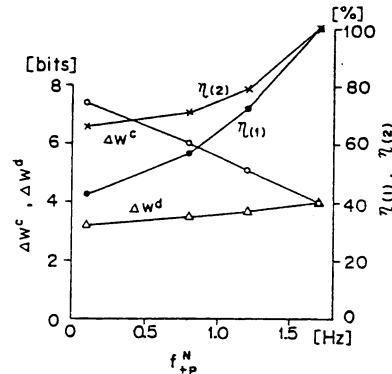
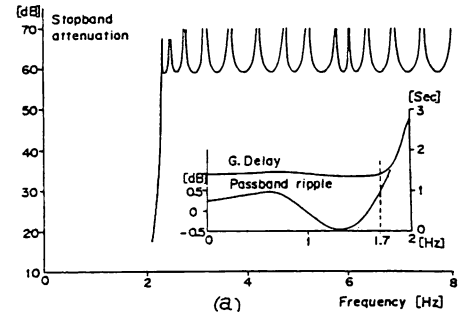


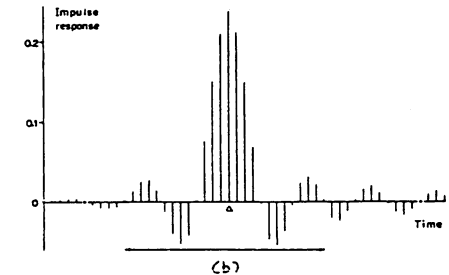
Fig. 5 Simulation for ΔW^C , ΔW^d , $\eta(1)$ and $\eta(2)$ in terms of f_{+p}^N .

Table 3 Design parameters.

Frequency Domain			
M	4	f_s	16.0 Hz
$N_n^{(1)}$	28	f_{+p}	1.7 Hz
$N_n^{(2)}$	7	f_c	2.3 Hz
N_d	3	f_{+p}^N	0.1 Hz
Time Domain			
Wave form center	23T, $T=1/16$ Sec		
Symmetrical condition	23±13T		



(a) Frequency responses.



(b) Time response.

Fig. 7 Designed filter responses. (a) Frequency responses. (b) Time response.

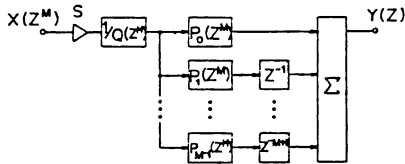


Fig. 2 Polyphase filter block-diagram

Table 1 Design parameters.

Frequency Domain			
M	16	f_s	64.0 Hz
$N_n^{(1)}$	80	f_{+p}	1.7 Hz
$N_n^{(2)}$	1	f_c	2.3 Hz
N_d	4	f_{+p}^N	0.1 Hz

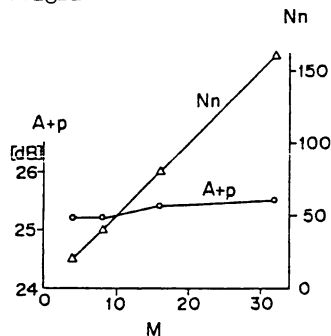


Fig. 3 Simulation for relation between A_{+p} and M_n .

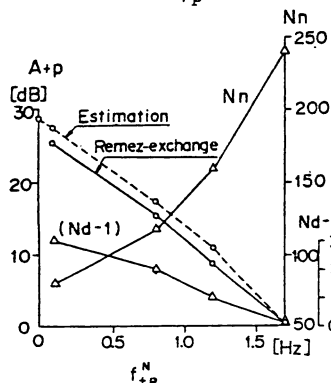


Fig. 4 Estimation and simulation for relation between A_{+p} and f_{+p}^N .

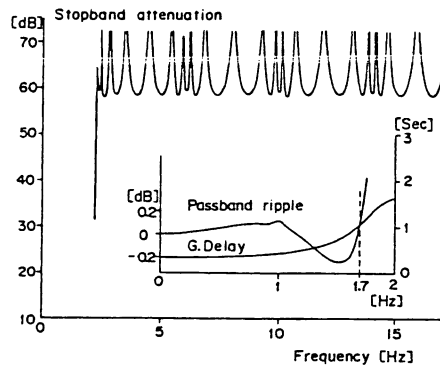


Fig. 6 Designed frequency responses.

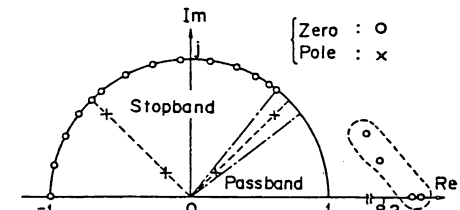


Fig. 8 Pole-zero locations.

Table 2 Circuit complexity comparison.

Parameters	FIR Filter	Bellanger's Method	Proposed Method
$N_n^{(1)}$	240	113	80
$N_n^{(2)}$		1	1
$N_d - 1$		7	3
$ Q(e^{j\omega_{+p}}) ^{-1}$	1	138.0	18.56
ΔW^C bits	4.0	10.6	7.4
ΔW^d bits	4.0	3.7	3.2
$\eta(1)$ %	100	76.3	42.6
$\eta(2)$ %	100	143	65.7
Average Delay Sec.	1.875	0.366	0.346

Table 4 Circuit complexity comparison.

Parameters	FIR Filter	Proposed Method
$N_n^{(1)}$	55	28
$N_n^{(2)}$		7
$N_d - 1$		2
$ Q(e^{j\omega_{+p}}) ^{-1}$	1	6.46
ΔW^C bits	2.9	5.25
ΔW^d bits	2.9	2.9
$\eta(1)$ %	100	79.6
$\eta(2)$ %	100	92.8
Average Delay Sec.	1.72	1.44